Geophysical Research Letters

RESEARCH LETTER
10.1029/2022GL098959

Constraints on the Role of Laplace Pressure in Multiphase Reactions and Viscosity of Organic Aerosols

Sarah S. Petters[1,2]

[1]Department of Environmental Sciences and Engineering, Gillings School of Global Public Health, The University of North Carolina at Chapel Hill, Chapel Hill, NC, USA, [2]Now at: Department of Chemistry, Aarhus University, Aarhus, Denmark

Key Points:

- An expression is formulated describing size-dependent aerosol reaction rates and viscosity by linking Köhler theory with organic chemistry
- Reactions of peroxides, epoxides, furans, aldols, carbonyls, and others are predicted to be up to tenfold faster in 3–10-nm particles
- Aerosol viscosity at the nanoscale varies as a function of the thermal properties, compressibility, and surface tension of the material

Supporting Information:

Supporting Information may be found in the online version of this article.

Correspondence to:

S. S. Petters,
spetters@unc.edu

Citation:

Petters, S. S. (2022). Constraints on the role of Laplace pressure in multiphase reactions and viscosity of organic aerosols. *Geophysical Research Letters*, *49*, e2022GL098959. https://doi.org/10.1029/2022GL098959

Received 31 MAR 2022
Accepted 12 MAY 2022

Author Contributions:

Conceptualization: Sarah S. Petters
Formal analysis: Sarah S. Petters
Funding acquisition: Sarah S. Petters
Investigation: Sarah S. Petters
Methodology: Sarah S. Petters
Project Administration: Sarah S. Petters
Supervision: Sarah S. Petters
Visualization: Sarah S. Petters
Writing – original draft: Sarah S. Petters
Writing – review & editing: Sarah S. Petters

Abstract Aerosol chemistry has broad relevance for climate and global public health. The role of interfacial phenomena in condensed-phase aerosol reactions remains poorly understood. In this work, liquid drop formalisms are coupled with high-pressure transition state theory to formulate an expression for predicting the size-dependence of aerosol reaction rates and viscosity. Insights from high-pressure synthesis studies suggest that accretion and cyclization reactions are accelerated in 3–10-nm particles smaller than 10 nm. Reactions of peroxide, epoxide, furanoid, aldol, and carbonyl functional groups are accelerated by up to tenfold. Effective rate enhancements are ranked as: cycloadditions >> aldol reactions > epoxide reactions > Baeyer-Villiger oxidation >> imidazole formation (which is inhibited). Some reactions are enabled by the elevated pressure in particles. Viscosity increases for organic liquids but decreases for viscous or solid particles. Results suggest that internal pressure is an important consideration in studies of the physics and chemical evolution of nanoparticles.

Plain Language Summary Airborne particles (aerosols) are ubiquitous and have broad relevance to climate and public health. Chemical reactions in particles can alter their volatility, light absorption, toxicity, and hygroscopicity. These reactions are difficult to characterize due to the difficulty of detecting interfacial phenomena and molecules in nanoparticles. This work derives an expression to predict changes in reaction rates and viscosity of nanoparticles; the expression is then used in conjunction with a survey of data from organic synthesis studies to make predictions relevant to atmospheric chemistry. Viscosity and reaction rates change due to constriction by the force of surface tension, which raises internal pressure. Concerted cyclization and accretion reaction rates were predicted to be enhanced; the net effect on multi-step reactions is inhibition. Incorporation of these insights into atmospheric chemistry changes the way we interpret activity and reactivity in the aerosol phase.

1. Introduction

Aerosols have far-reaching impacts including adverse health effects, reduction in visibility, modification of clouds, and alteration of the Earth's climate. Aerosols affect climate by absorbing or scattering solar radiation, regulating condensation and evaporation of atmospheric trace gases including water, and affecting cloud properties by serving as cloud condensation nuclei (CCN). The substantial role of aerosols in the hydrological cycle is a significant source of uncertainty in climate projections (Forster et al., 2021).

Nucleation and growth of new particles is the major contributor to both particle number and CCN-active particles in the atmosphere (H. Gordon et al., 2017; Kulmala et al., 2004; Pierce et al., 2011). The role of organic molecules in the nucleation mechanism is not precisely known (Kürten et al., 2016). Nucleation occurs when a nascent molecular cluster achieves a diameter exceeding ∼0.7–1.7 nm and condensation of additional molecules becomes energetically favorable (Sipilä et al., 2010). New particle formation has been observed in various environments and occurs through different chemical pathways (Kerminen et al., 2018; Kulmala et al., 2004). Although nucleation is driven by the condensation of low-volatility inorganic species such as sulfuric acid, amines, iodic acid, and nitric acid (Baccarini et al., 2020; Kurtén et al., 2008; O'Dowd et al., 2002; Sipilä et al., 2016; Wang et al., 2020; Yao et al., 2018; Zhao et al., 2011), organic molecules can also contribute (Brean et al., 2020; Fang et al., 2020; Kirkby et al., 2016). Further, condensation of organics is necessary for particle growth from ∼3 nm toward 50–100 nm, where they may serve as CCN (Donahue et al., 2011; Mohr et al., 2019; Tröstl et al., 2016). Despite their ubiquity, the composition and volatility of organic molecules involved in particle formation and growth remain difficult to characterize (Bianchi et al., 2019; Glasius & Goldstein, 2016).

Though condensed-phase reactions have a substantial influence on atmospheric organic chemistry (Herrmann et al., 2015; Su et al., 2020), these reactions remain largely unexplored. The aerosol matrix is partly to blame. Aerosol phases can include, for example, liquids, phase-separated liquids (Rastak et al., 2017; Renbaum-Wolff et al., 2016), viscous semisolids (S. S. Petters et al., 2019; Renbaum-Wolff et al., 2013; Virtanen et al., 2010), crystalline solids, and the surface phase (Enami et al., 2017; Eugene et al., 2018; Wei et al., 2018). Water is generally present in atmospheric particles and controls aerosol pH and heterogeneous reaction rates (Ervens et al., 2011; T. B. Nguyen et al., 2014; Pye et al., 2020). Aerosol viscosity is thought to play a critical role in determining nucleation and growth rates, but the processes involved are not yet fully understood (Reid et al., 2018). Careful application of experimental, observational, and modeling insights is needed to understand how nanoscale phase controls heterogeneous reactions.

The size-dependent aerosol surface-to-volume ratio and Laplace pressure become especially important at the nanoscale. M. D. Petters and Kasparoglu (2020) and Cheng et al. (2015) explore the size-dependence changes to aerosol viscosity induced by surface tension (Kaptay, 2012). Riva et al. (2021) explore the pressure dependence of imidazole formation in aerosols. The present work fills gaps in (1) the development of thermodynamic formalisms describing the pressure-induced diameter dependence of particle-phase (a) reaction rates, and (b) viscosity; and (2) evidence and application of interdisciplinary high-pressure sciences to atmospheric organic chemistry.

2. Theoretical Development

Surface tension raises the vapor pressure adjacent to a curved liquid surface relative to its Clausius-Clapeyron or Arrhenius temperature dependence; this effect is described by the Kelvin equation for pure liquids and by Köhler theory for mixtures, for example, (Bilde et al., 2015; Kreidenweis et al., 2005):

$$S_i = a_i exp\left(\frac{4\sigma v_i}{RTD}\right), \tag{1}$$

where subscript i denotes the ith component, S_i is the vapor pressure outside the interface, a_i is activity, σ is surface tension, v_i is molar volume, R is the universal gas constant, T is temperature, and D is diameter; this is the Köhler equation when i = water. Laplace pressure, Δp_L, is the pressure inside a droplet resulting from intermolecular forces and the interfacial curvature: $\Delta p_L = 2\sigma/r + d\sigma/dr$, where r is the droplet radius. A volumeless surface interface is assumed and is defined by the radius-of-tension, r_t, for which $d\sigma/dr = 0$, yielding (Laaksonen et al., 1999; Pruppacher & Klett, 2010; Rowlinson & Widom, 1982):

$$\Delta p_L = 2\sigma/r_t. \tag{2}$$

Laplace pressure keeps the condensate in mechanical equilibrium with the gas and is equivalent to $4\sigma/D$ in Köhler theory.

Figure 1 (panel a) estimates Laplace pressure in 3–500 nm particles using Equation 2 for surface tensions corresponding to highly concentrated aqueous salt slurries (0.080 N m^{-1}; S. S. Petters & Petters, 2016; Su et al., 2020), water (0.072 N m^{-1}), and pure organic liquid or concentrated aqueous surfactant (0.030 N m^{-1}; Hritz et al., 2016; Korosi & Kovats, 1981; Petters &. Petters, 2016). For 3–10 nm particles, Δp_L is ∼100–10 MPa. For 50–100 nm particles, Δp_L is ∼6–1 MPa. Reduced atmospheric pressure aloft alters these values by a negligible fraction. Laplace pressure in a 3-nm particle is 400–1000× higher than that of the same material in bulk.

Is this a remarkable pressure? Figure 1 (panels b–d) compares particle internal pressures to pressures encountered in high-pressure chemistry, analytical chemistry, oceanography, and geology. Though aerosol internal pressure is too low to inactivate pathogens (Figure 1, panel c), capillary forces in the microscale could be important to bioaerosol viability (McRae et al., 2021). Pressures in particles 3–10 nm in diameter are close to those encountered in medium-to high-pressure synthetic organic chemistry, liquid chromatography, the ocean depths, and subsurface drilling.

How, then, does pressure affect reaction rates? The pressure dependence of a reaction rate constant, $\partial ln(k)/\partial p$, is derived from the free energy change during compression (Evans & Polanyi, 1936; Van Eldik & Kelm, 1980):

$$\Delta ln(k) = -\Delta p_{rxn}\Delta V^{\ddagger}/RT \tag{3}$$

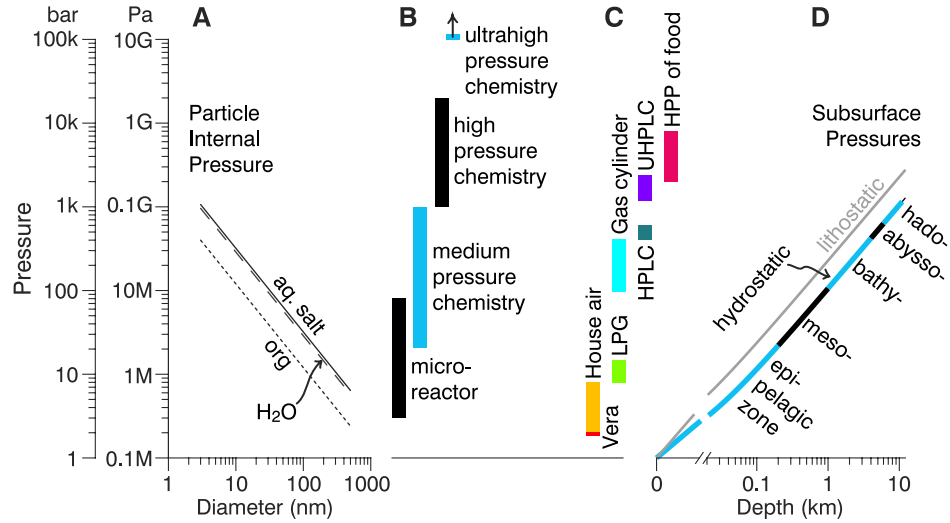

Figure 1. (a) Particle internal pressure for diameters of 3–500 nm, Δp_L (Equation 1), using surface tensions of 0.08 (aqueous salts), 0.072 (water), and 0.03 N m^{-1} (organic). (b) Pressure ranges used in high-pressure chemistry (Benito-López et al., 2008). (c) Pressures encountered in analytical chemistry and food processing. Vera = VOAG (Vibrating Orifice Aerosol Generator) evaporation and residual analysis (S. S. Petters et al., 2020). House air = laboratory compressed air. LPG = liquefied petroleum gas. HPLC = high-performance liquid chromatography. UHPLC = ultrahigh-performance liquid chromatography. HPP = high-pressure Pasteurization of foods (Demazeau & Rivalain, 2011; Grove et al., 2006; Kovač et al., 2010). (d) Pressures encountered in oceanography, geomicrobiology, and petroleum geology; the lithostatic gradient is 22.7 MPa km^{-1} and the hydrostatic gradient is 10.5 MPa km^{-1} (Tiab & Donaldson, 2016). Pressures are absolute; *y*-axes apply to all panels.

where $k = k_p/k_0$ is the rate enhancement factor, k_p is the rate constant at high pressure, k_0 is the rate constant at the reference pressure, Δp_{rxn} is the experimental gauge pressure, and $\Delta V^{\ddagger}$ is the change in volume of the reaction transition state. The quantity $\Delta V^{\ddagger}$ is parameterizes the pressure dependence of reaction rates in high-pressure synthesis. Reactions are accelerated under pressure if they decrease in volume during the transition state, $\Delta V^{\ddagger} < 0$; reactions with a positive $\Delta V^{\ddagger}$ proceed more slowly (Klärner & Wurche, 2000). Cyclic transition states in concerted rearrangements tend to have lower $\Delta V^{\ddagger}$ than acyclic intermediates in stepwise reactions (Van Eldik & Hubbard, 1997). Bond-breaking and neutralization reactions tend to have positive $\Delta V^{\ddagger}$, and bond-forming and ionogenic reactions tend to have negative $\Delta V^{\ddagger}$; this is due to relaxation or constriction of the solvent cage (Isaacs, 1997). For this reason, the volume $\Delta V^{\ddagger}$ is often split into intrinsic and the solvent-dependent molar volumes: $\Delta V^{\ddagger} = \Delta V^{\ddagger}_{intr} + \Delta V^{\ddagger}_{solv}$. Experimentally determined $\Delta V^{\ddagger}$ ranges are compiled below.

The Laplace and Evans-Polanyi expressions are here combined. Setting Δp_L equal to Δp_{rxn} yields an expression describing the reaction rate change due to the aerosol Laplace pressure:

$$\frac{k_p}{k_0} = exp\left(\frac{-4\sigma\Delta V^{\ddagger}}{RTD}\right). \quad (4)$$

Equation 4 is not an extension of Köhler theory (Equation 1); rather, the remarkable similarity between Equations 1 and 4 is due to their similar thermodynamics. Equation 1 is based on chemical equilibrium across phase boundaries and Equation 3, from which Equation 4 is derived, is based on chemical equilibrium between reactants and the transition state.

Viscosity is altered under high hydrostatic pressure, changing diffusion and vibration timescales and contributing to changes in observed reaction rates. The relationship between $\Delta ln(k)$ and Δp_{rxn} becomes nonlinear as pressure becomes high (Chen et al., 2017). A rate constant expression accounting for viscosity is derived by Sumi (1991): $k_{p'}^{-1} = k_p^{-1} + k_v^{-1}$; k_p is given in Equation 4 and k_v is proportional to $\eta^{-0.7}$, where η is viscosity. Incorporating viscosity into Equation 4,

$$1/k_{p'} = \exp\left(\frac{4\sigma\Delta V^{\ddagger}}{RTD}\right)/k_0 + \eta^{0.7}/c, \tag{5}$$

where c is a proportionality constant.

The isothermal pressure dependence of viscosity is predicted using the isothermal compressibility ($\kappa_{T,\xi}$) and isobaric thermal expansion coefficient ($\alpha_{p,\xi}$) (Schmelzer et al., 2005):

$$\left(\frac{\partial\eta}{\partial p}\right)_{T,\xi} = -\frac{\kappa_{T,\xi}(p,T,\xi)}{\alpha_{p\xi}(p,T,\xi)}\left(\frac{\partial\eta}{\partial T}\right)_{p,\xi} \tag{6}$$

where p is pressure, ξ is a state variable describing the molecular-level order of the mixture (Schmelzer et al., 2011), and $(\partial\eta/\partial T)_{p,\xi}$ is the slope of $\eta(T)$ at constant pressure. This last term, the temperature-dependent viscosity $\eta(T)$, is predicted using the Vogel–Fulcher–Tammann (VFT) equation: $\log_{10}\eta = A + B/(T - T_0)$; A, B and T_0 are fitted (Fulcher, 1925). Incorporation of the VFT slope into Equation 6 yields the pressure dependence of viscosity:

$$\left(\frac{\partial\eta}{\partial p}\right)_{T,\xi} = \frac{\kappa_{T,\xi}(p,T,\xi)}{\alpha_{p,\xi}(p,T,\xi)}\frac{B\ln(10)}{(T-T_0)^2}\,10\hat{}\left(A + \frac{B}{T-T_0}\right). \tag{7}$$

Equation 7 indicates that in the absence of changes in the microstructural order (including phase change), viscosity always increases with pressure. Equations 1–4 are used for liquid mixtures and Equations 5–7 become important at higher viscosities.

3. Discussion

Surface tension, the defining parameter in Equations 1–5, is uncertain for aerosols. Prior work on aerosol surface tension has largely been undertaken in the context of nucleation (Equation 1). Interfacial tension determines the energetic barrier to creating additional surface area and is therefore important not only in theoretical descriptions of new particle formation (Laaksonen et al., 1999), but also in CCN activation (S. S. Petters & Petters, 2016; Wex, Stratmann, Topping, & McFiggans, 2008) and the properties of cloud droplets (Dufour & Defay, 1963; Pruppacher & Klett, 2010). CCN activation theory and measurements have been used to understand surface tension at the nano- and microscale (Bzdek et al., 2020; Facchini et al., 1999; Forestieri et al., 2018; Nozière et al., 2014; Ovadnevaite et al., 2017; S. S. Petters & Petters, 2016; Prisle et al., 2008; Ruehl et al., 2016; Wex, Stratmann, Topping, & McFiggans, 2008). The growing consensus suggests that the surface tension is not inherently size-dependent, but that the activity term (a_i) must be accurately known to estimate the surface tension of nanoparticles smaller than ~100 nm from CCN activation data (Malila & Prisle, 2018; McGraw & Wang, 2021; M. D. Petters & Kreidenweis, 2013; Prisle et al., 2008). The implication of these studies is that nanoparticle surface tension depends in part on the phase state of the particle bulk.

Direct measurement of particle surface tension at the nanoscale has not been possible. However, simulations and microscale measurements can shed light on the surface tension at the nanoscale. Molecular dynamics simulations of liquid water in 1–2-nm nanopores indicate that the Young-Laplace equations are accurate at that scale, though tension was reduced (0.072–0.062 N m^{-1}) (Liu & Cao, 2016). Molecular dynamics simulations of atmospherically relevant organic surfactants in 5-nm droplets are in good agreement with bulk measurements (Hede et al., 2011). Bzdek et al. (2020) used aerosol optical tweezers to confirm experimentally that the surface tension of 10-μm droplets containing strong surfactants is close to that of bulk measurements. Although direct evidence is limited, it is expected that the Laplace pressure predicted by Equations 1 and 2 is valid in particles larger than ~1 nm in diameter.

Figure 2 shows rate changes for atmospheric aerosol reactions estimated using known $\Delta V^{\ddagger}$ values. Panel A summarizes $\Delta V^{\ddagger}$ for a broad range of reactions. Data sources are as follows. The majority of values were transcribed from the review of Isaacs (1997). For a more generalized review based on mechanistic features, see Chen et al. (2017). Benito-López et al. (2008) provide a $\Delta V^{\ddagger}$ range for [2,2]-cycloaddition consistent with that of Isaacs, albeit narrower; the Isaacs range of −55 to −40 cm^3 mol^{-1} is displayed. For a density of 1.4–1.65 g cm^{-3} representative of SOA or biomass burning SOA (Kristensen et al., 2021; Nakao et al., 2013) and a molar mass of ~250 g mol^{-1} (Hodzic et al., 2010), every 10 cm^3 mol^{-1} of $\Delta V^{\ddagger}$ corresponds to 5.6%–6.6% of the molar volume. Yamashita et al. (2014) report high-pressure yields for lactone polymerization; the apparent rate constant after assuming a first-order reaction

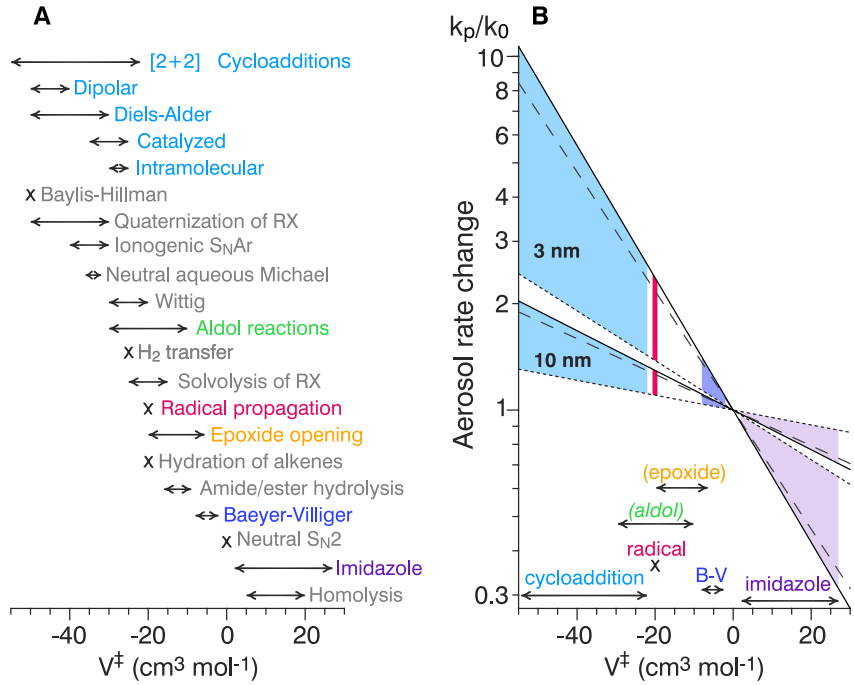

Figure 2. (a) Ranges in $\Delta V^{\ddagger}$ for reactions from the high-pressure organic synthesis literature. Data sources described in the text. Atmospherically-relevant reactions are given in color (cycloaddition: blue; aldol: green; radical: magenta; epoxide: gold; Baeyer-Villiger: indigo; imidazole: purple); other reactions are gray. (b) Calculated change in reaction rate due to particle internal pressure (Equation 4), for 3- and 10-nm particles, as a function of the transition state volume, $\Delta V^{\ddagger}$. Surface tensions of 0.08, 0.072, and 0.03 N m^{-1} are assumed (solid, dashed, and dotted lines). Color-shaded regions trace out the uncertainty in rate change based on uncertainty in $\Delta V^{\ddagger}$ and in surface tension (colors correspond to $\Delta V^{\ddagger}$ ranges in panel A; select ranges are reprinted below the graph in panel b).

is used here with Equation 3 to produce an effective $\Delta V^{\ddagger}$ of -7 cm^3 mol^{-1}. For ring-opening of propylene oxide, isobutylene oxide, and ethylene oxide, Koskikallio and Whalley (1959) report a $\Delta V^{\ddagger}$ range of -9.2 to -6 cm^3 mol^{-1}. The $\Delta V^{\ddagger}$ range for epoxide ring-opening of Isaacs is -20 to -15 cm^3 mol^{-1}, which is extended to -6 cm^3 mol^{-1} here to include the Yamashita and Koskikallio and Whalley results. The neutral aqueous Michael reaction of methyl vinyl ketone with nitromethane was conducted by Jenner (1999), who used the effective pseudo-second-order rate expression with Equation 3 to obtain the effective $\Delta V^{\ddagger}$ range of -32 to -35 cm^3 mol^{-1} Jenner (2001) report a $\Delta V^{\ddagger}$ range of -2 to -8 cm^3 mol^{-1} for a series of Bayer-Villiger reactions of peroxy acids with ketones, concluding that the reaction is concerted. The imidazole reaction of glyoxal with ammonium sulfate at different solution ionic strengths is described by Riva et al. (2021). Equation 3 is used here with an assumed pseudo-first-order rate of polymerization, quantified using light absorption, to calculate the effective $\Delta V^{\ddagger}$ range of 2–27 cm^3 mol^{-1}. Due to the multi-step nature of many of the reactions presented (e.g., imidazole formation, Michael addition, ring-opening polymerization), $\Delta V^{\ddagger}$ is an observed quantity variously referred to as effective, pseudo, or semi-empirical.

Figure 2 (panel b) summarizes expected changes in reaction rates in particles of 3 and 10 nm diameters based on Equation 4. Color regions trace the uncertainty for different types of reactions from panel (a). For cycloadditions (blue region), the potential impact of particle internal pressure is the highest and results in the maximum rate change factor of 10 in 3-nm particles with high salt content ($\sigma \sim 0.08$ N m^{-1}). The imidazole reaction (purple region) results in a rate change factor of as low as 0.3 in 3-nm particles with high salt content, for example, a 70% reduction in rate. For diameters larger than 3 nm, reactions with smaller absolute $\Delta V^{\ddagger}$ values, or surface tensions lower than 0.08 N m^{-1}, rate change factors trend away from these extremes toward unity. For example, the magenta bar in Figure 2 (panel b) traces the uncertainty in k_p/k_0 for condensed-phase radical propagation reactions ($k_p/k_0 \sim 1.1$–2.4). Radical propagation in atmospheric chemistry is most commonly understood as the key step in oxidation (Ehn et al., 2014; Matsunaga & Ziemann, 2010; Ziemann & Atkinson, 2012). Similar propagation reactions of peroxy radicals also occur in condensed-phase organic matrices (Ingold, 1961) and in fog and cloud droplets (Lim et al., 2010). Aldol and epoxide reactions are not shaded due to their overlap with other

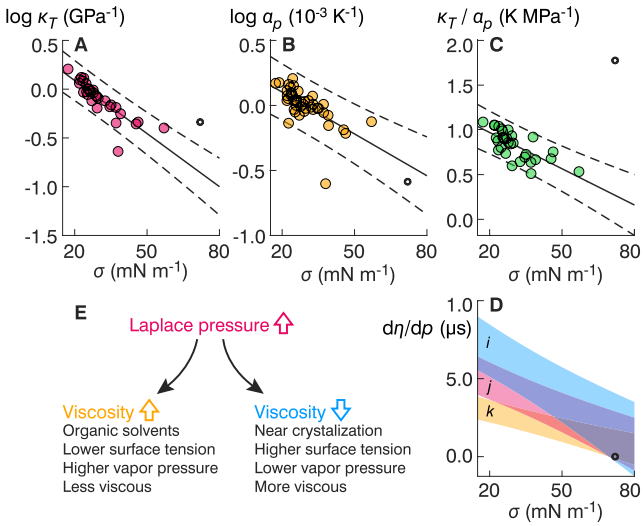

Figure 3. Predicted trend in viscosity with increasing pressure for a series of organic liquids. *X*-axis: surface tension at 298.15 (K) (a) Isothermal compressibility. (b) Isobaric coefficient of thermal expansion. (c) Ratio κ_T/α_p. Open black circle: water (Schmelzer et al., 2005). Solid lines: best fit; Dotted lines: 95% CI. (d) Predicted slope of viscosity as a function of pressure assessed at 298.15 K and atmospheric pressure for a slope $d\eta/dT$ (Pa s K^{-1}) for (i) 2.5%, (j) 5%, and (k) 10% sucrose in water (Kasparoglu et al., 2021; Rothfuss & Petters, 2017). Shaded regions reflect uncertainty in κ_T/α_p (panel c). (e) Predicted trend for atmospheric aerosols.

chart elements (Figure 2, panel b) but have a k_p/k_0 of 1.05–3.4 and 1.02–2.4, respectively. Baeyer-Villiger oxidations have a k_p/k_0 of 1.01–1.4.

Figure 3 shows the trend in aerosol viscosity with increasing internal pressure based physicochemical properties. Panel (a) compares compressibility, $\kappa_{T,\xi}$, with organic surface tension, following Richard and Rogers (1971). Data are obtained for organic liquids with the formula $C_xH_yO_z$ at 298 K from (Marcus, 1998; Yaws, 2003; taken from; Caleman et al., 2012). Panels (b) and (c) extend the linear surface tension dependence to $\alpha_{p,\xi}$ and $\kappa_{T,\xi}/\alpha_{p,\xi}$. Panel (d) shows the range in pressure-dependent viscosity predicted by Equation 7. Ranges are calculated from predicted $\kappa_{T,\xi}/\alpha_{p,\xi}$ values (panel c). Calculations are made for 2.5%, 5%, and 10% sucrose in water (regions *i*, *j*, and *k*, respectively) following the detailed model of Kasparaglu et al. (2021). This model is based on liquids far from phase transition, and $d\eta/dp$ is always positive. Analogous to water melting under pressure, atmospheric aerosols are predicted to become less viscous at ultrafine sizes (Panel E) (Cheng et al., 2015; M. Petters & Kasparoglu, 2020). Experimental $d\eta/dT$ measurements for viscous atmospherically-relevant aerosols demonstrate a wider range of values indicative of more complex mixtures (Table S1 in Supporting Information S1) (Marsh et al., 2018; S. S. Petters et al., 2019; Rothfuss & Petters, 2017).

4. Implications for Multiphase Atmospheric Chemistry

This work combines the Laplace and Evans-Polyani expressions for application to atmospheric chemistry. It is predicted that all particle-phase reactions are affected by particle internal pressure as a function of particle diameter ($D < \sim$10 nm), surface tension, effective $\Delta V^{\ddagger}$, and pressure-induced changes in aerosol phase state. The following explores the effects of Laplace pressure on known reaction systems. The estimates presented here can then serve to start the discussion of reactions of similar highly functionalized molecules in nucleating or evaporating nanoparticles.

Highly oxygenated molecules (HOMs) are a class of low molecular weight compounds that participate in both nucleation and subsequent particle growth (Ehn et al., 2014). HOMs (e.g., multifunctional peroxides) can serve as oxidants in condensed-phase Baeyer-Villiger reactions, in which hydroperoxides or peroxyacids oxidize aldehydes or ketones. Bayer-Villiger reactions have a slightly negative $\Delta V^{\ddagger}$ and have been observed in chamber experiments (Claflin et al., 2018) and in the field (Pospisilova et al., 2020). Because HOMs are an important early participant in new particle growth, they are likely present in 3–10-nm particles (Bianchi et al., 2019). Thus, pressure likely provide moderate enhancement of peroxide depletion rates and higher carboxylic acids yields, similar to the observations of Pospisilova et al.

Epoxides, for example, α-lactones, are important oxidation products of biogenically-derived hydroperoxides. Isoprene-derived epoxydiols (Paulot et al., 2009; Surratt et al., 2010) and α-pinene derived epoxides (Eddingsaas et al., 2012) form photochemically under low-NO conditions. Under high-NO conditions, formation of isoprene-derived hydroxymethyl-methyl-α-lactone (T. B. Nguyen et al., 2015; Surratt et al., 2010) and methacrylic acid epoxide (Lin et al., 2013) is observed. Epoxides undergo acid-catalyzed ring-opening reactions in the aerosol, contributing up to 14%–40% of organic aerosol mass in forested regions (Budisulistiorini et al., 2015; Froyd et al., 2010; W. W. Hu et al., 2015; Schulz et al., 2018; Xu et al., 2015). Ring-opening rates and mechanisms are guided by solution pH and ionic strength (Eddingsaas et al., 2010; Lin et al., 2013; T. B. Nguyen et al., 2014; S. S. Petters et al., 2021). High hydrostatic pressure has been used to differentiate between the S_N1 and S_N2 reaction pathways for epoxides (Baliga & Whalley, 1964; Whalley, 1959). Structural features play an important role in both the rate and the mechanism of epoxide reactions (Eddingsaas et al., 2010; Minerath & Elrod, 2009; S. S. Petters et al., 2021), meaning that the effect of particle internal pressure is compound-specific. For example, the multi-step ammonium-catalyzed reaction of isoprene-derived epoxydiols at high pH (Nozière et al., 2018) may proceed more slowly at elevated pressure, analogous to the result of Riva et al. (2021) for glyoxal reacting

with ammonium. The five-membered lactone, γ-butyrolactone, undergoes acid-catalyzed ring-opening reactions exclusively under high hydrostatic pressure due to the stability of its ring structure at lower pressures (Houk et al., 2008; Yamashita et al., 2014).

Furanoic compounds are an important group of five-membered aromatic heterocyclic gases emitted during biomass burning (Hartikainen et al., 2018). New particle formation is observed in biomass burning plumes during photochemical oxidation (Hennigan et al., 2012). The uptake of furans by aerosols and hydrometeors can result in condensed-phase reactions adding to particulate mass (Liang et al., 2018; Tomaz et al., 2018). Diels-Alder cycloadditions of furans with alkenes have enhanced yields under high pressure, due in part to the prevention of thermally-accelerated reverse reactions (Dauben & Krabbenhoft, 1976; Isaacs, 1997; Oppolzer, 1991). Furanoic compounds present during the growth of these new particles can partition into the condensed phase and experience elevated pressures. Note that in-flame nucleation and soot formation results in particles greater than ∼10 nm (Johansson et al., 2018); nanosphere soot and tarballs have diameters of ∼50 and ∼250 nm, respectively (Adachi et al., 2019). Though compaction of soot occurs by capillary forces (Bhandari et al., 2019; D. Hu et al., 2021; Leung et al., 2017; Ma et al., 2013), the pressure in these accumulation-mode particles is also outside the range for which condensed-phase reaction rates are altered (Figure 1, panel a). Given that cycloadditions including the Diels-Alder reaction are the most dramatically accelerated by increased pressure, oligomerization of furanoid compounds during the nucleation and growth of new particles in sunlit biomass burning plumes is likely affected by particle internal pressure.

Carbonyls such as pyruvic acid and glyoxal are highly water-soluble and can dimerize (Loeffler et al., 2006; Perkins et al., 2016) or undergo multi-step oligomerization in the presence of ammonium (Maxut et al., 2015). Riva et al. (2021) show that high hydrostatic pressure reduces the oligomerization rate of glyoxal in the presence of ammonium sulfate. Pyruvic acid undergoes imidazole formation and this reaction rate is likely reduced in the nucleation-mode aerosol. Hazen et al. (2002) show that pyruvic acid decarboxylates under pressure to form acetic acid and carbon dioxide and undergoes aldol condensation to form dimers and trimers; a large fraction of these decarboxylate to form methyl succinate, and some undergo Diels-Alder cyclization. Pyruvic acid dimers are important in atmospheric chemistry because they are surface-active (B. P. Gordon et al., 2019; Hazen et al., 2002) and cyclize in droplets (Perkins et al., 2016; S. S. Petters et al., 2020). Aldol reactions are a hypothesized route for reactive uptake of gases or modification of aerosol optical properties when catalyzed by inorganic salts (Nozière et al., 2010), and have been suggested for highly acidic particles and in evaporating droplets (De Haan et al., 2009; Herrmann et al., 2015; Jang et al., 2002).

Characterization of molecules and reaction mechanisms in aerosols is challenging and often informed by studies of bulk samples at standard temperature and pressure (Glasius & Goldstein, 2016). Higher pressures may enable the formation of different reaction products. For example, high pressure can prevent backwards reactions or enable otherwise-unfavorable ring-opening reactions. This work adjusts the existing assumptions of aerosol phase state, opening the door for future and retrospective studies seeking to match observations to reaction models.

Aerosol viscosity is predicted to change due to Laplace pressure. Organic solvents become more viscous under pressure (Cook et al., 1994; Herbst et al., 1993; Isaacs, 1997). In contrast, supercooled water becomes less viscous as the hydrogen bond network collapses (∼300 MPa) (Singh et al., 2017). Further, melting points of various organic and inorganic substances are depressed in sub-100-nm particles (M. D. Petters & Kasparoglu, 2020), and secondary organic aerosols below 20 nm are predicted to liquefy (Cheng et al., 2015).

5. Conclusions

This work combines thermodynamics from aerosol physics and organic physical chemistry to formulate expressions for the diameter-dependent reaction rates and viscosity in particles. Application of this equation is guided by a survey of synthetic organic chemistry and suggests that heterogeneous reaction rates are accelerated by up to tenfold in 3–10-nm particles. Elevated pressure is explored as a primary contributor to size-dependent reaction rates and mechanisms of HOMs and other peroxides, furans and furanoids, epoxides and other lactones, and carbonyls. Rate enhancements are ranked as follows: cycloadditions >> aldol reactions > epoxide ring-opening reactions > Baeyer-Villiger oxidation by peroxides >> imidazole oligomerization of carbonyls. High-pressure changes to aerosol viscosity depend on aerosol composition and temperature. Careful work is needed to separate

the effects of particle internal pressure, viscosity, curvature, pH, phase separation, surface tension, and other factors on reactions within particles.

Data Availability Statement

Data are archived on Zenodo at https://doi.org/10.5281/zenodo.6546580.

Acknowledgments
This project was funded by the U.S. National Science Foundation Postdoctoral Fellowship Award #AGS-1624696. SSP thanks Merete Bilde, Lærke Nielsen, Markus Petters, Tina Šantl-Temkiv, Torben Sigsgaard, and Yuzhi Chen for helpful discussions.

References

Adachi, K., Sedlacek, A. J., Kleinman, L., Springston, S. R., Wang, J., Chand, D., et al. (2019). Spherical tarball particles form through rapid chemical and physical changes of organic matter in biomass-burning smoke. *Proceedings of the National Academy of Sciences U.S.A*, *116*(39), 19336–19341. https://doi.org/10.1073/pnas.1900129116

Baccarini, A., Karlsson, L., Dommen, J., Duplessis, P., Vüllers, J., Brooks, I. M., et al. (2020). Frequent new particle formation over the high Arctic pack ice by enhanced iodine emissions. *Nature Communications*, *11*(1), 4924. https://doi.org/10.1038/s41467-020-18551-0

Baliga, B. T., & Whalley, E. (1964). Effect of pressure on the acid-catalyzed enolization of acetone and acetophenone in various ethanol-water solvents. Origin of the enthalpy-entropy compensation effect. *Canadian Journal of Chemistry*, *42*(8), 1835–1850. https://doi.org/10.1139/v64-275

Benito-López, F., Egberink, R. J. M., Reinhoudt, D. N., & Verboom, W. (2008). High pressure in organic chemistry on the way to miniaturization. *Tetrahedron*, *64*(43), 10023–10040. https://doi.org/10.1016/j.tet.2008.07.108

Bhandari, J., China, S., Chandrakar, K. K., Kinney, G., Cantrell, W., Shaw, R. A., et al. (2019). Extensive soot compaction by cloud processing from laboratory and field observations. *Scientific Reports*, *9*(1), 11824. https://doi.org/10.1038/s41598-019-48143-y

Bianchi, F., Kurtén, T., Riva, M., Mohr, C., Rissanen, M. P., Roldin, P., et al. (2019). Highly oxygenated organic molecules (HOM) from gas-phase autoxidation involving peroxy radicals: A key contributor to atmospheric aerosol. *Chemical Reviews*, *119*(6), 3472–3509. https://doi.org/10.1021/acs.chemrev.8b00395

Bilde, M., Barsanti, K., Booth, M., Cappa, C. D., Donahue, N. M., Emanuelsson, E. U., et al. (2015). Saturation vapor pressures and transition enthalpies of low-volatility organic molecules of atmospheric relevance: From dicarboxylic acids to complex mixtures. *Chemical Reviews*, *115*(10), 4115–4156. https://doi.org/10.1021/cr5005502

Brean, J., Beddows, D. C. S., Shi, Z., Temime-Roussel, B., Marchand, N., Querol, X., et al. (2020). Molecular insights into new particle formation in Barcelona, Spain. *Atmospheric Chemistry and Physics*, *20*(16), 10029–10045. https://doi.org/10.5194/acp-20-10029-2020

Budisulistiorini, S. H., Li, X., Bairai, S. T., Renfro, J., Liu, Y., Liu, Y. J., et al. (2015). Examining the effects of anthropogenic emissions on isoprene-derived secondary organic aerosol formation during the 2013 Southern Oxidant and Aerosol Study (SOAS) at the Look Rock, Tennessee ground site. *Atmospheric Chemistry and Physics*, *15*(15), 8871–8888. https://doi.org/10.5194/acp-15-8871-2015

Bzdek, B. R., Reid, J. P., Malila, J., & Prisle, N. L. (2020). The surface tension of surfactant-containing, finite volume droplets. *Proceedings of the National Academy of Sciences U.S.A.*, *117*(15), 8335–8343. https://doi.org/10.1073/pnas.1915660117

Caleman, C., Van Maaren, P. J., Hong, M., Hub, J. S., Costa, L. T., & Van der Spoel, D. (2012). Force field benchmark of organic liquids: Density, enthalpy of vaporization, heat capacities, surface tension, isothermal compressibility, volumetric expansion coefficient, and dielectric constant. *Journal of Chemical Theory and Computation*, *8*(1), 61–74. https://doi.org/10.1021/ct200731v

Chen, B., Hoffmann, R., & Cammi, R. (2017). The effect of pressure on organic reactions in fluids—A new theoretical perspective. *Angewandte Chemie International Edition*, *56*(37), 11126–11142. https://doi.org/10.1002/anie.201705427

Cheng, Y., Su, H., Koop, T., Mikhailov, E., & Pöschl, U. (2015). Size dependence of phase transitions in aerosol nanoparticles. *Nature Communications*, *6*(1), 5923. https://doi.org/10.1038/ncomms6923

Claflin, M. S., Krechmer, J. E., Hu, W. W., Jimenez, J. L., & Ziemann, P. J. (2018). Functional group composition of secondary organic aerosol formed from ozonolysis of α-pinene under high VOC and autoxidation conditions. *ACS Earth and Space Chemistry*, *2*(11), 1196–1210. https://doi.org/10.1021/acsearthspacechem.8b00117

Cook, R. L., King, H. E., Herbst, C. A., & Herschbach, D. R. (1994). Pressure and temperature dependent viscosity of two glass forming liquids: Glycerol and dibutyl phthalate. *The Journal of Chemical Physics*, *100*(7), 5178–5189. https://doi.org/10.1063/1.467276

Dauben, W. G., & Krabbenhoft, H. O. (1976). Organic reactions at high pressure. Cycloadditions with furans. *Journal of the American Chemical Society*, *98*(7), 1992–1993. https://doi.org/10.1021/ja00423a071

De Haan, D. O., Corrigan, A. L., Tolbert, M. A., Jimenez, J. L., Wood, S. E., & Turley, J. J. (2009). Secondary organic aerosol formation by self-reactions of methylglyoxal and glyoxal in evaporating droplets. *Environmental Science & Technology*, *43*(21), 8184–8190. https://doi.org/10.1021/es902152t

Demazeau, G., & Rivalain, N. (2011). The development of high hydrostatic pressure processes as an alternative to other pathogen reduction methods. *Journal of Applied Microbiology*, *110*(6), 1359–1369. https://doi.org/10.1111/j.1365-2672.2011.05000.x

Donahue, N. M., Trump, E. R., Pierce, J. R., & Riipinen, I. (2011). Theoretical constraints on pure vapor-pressure driven condensation of organics to ultrafine particles. *Geophysical Research Letters*, *38*(16), a–n. https://doi.org/10.1029/2011GL048115

Dufour, L., & Defay, R. (1963). *Thermodynamics of clouds*. Academic Press. Retrieved from https://catalog.lib.ncsu.edu/catalog/NCSU173811

Eddingsaas, N. C., Loza, C. L., Yee, L. D., Seinfeld, J. H., & Wennberg, P. O. (2012). α-pinene photooxidation under controlled chemical conditions – Part 1: Gas-phase composition in low- and high-NOx environments. *Atmospheric Chemistry and Physics*, *12*(14), 6489–6504. https://doi.org/10.5194/acp-12-6489-2012

Eddingsaas, N. C., VanderVelde, D. G., & Wennberg, P. O. (2010). Kinetics and products of the acid-catalyzed ring-opening of atmospherically relevant butyl epoxy alcohols. *The Journal of Physical Chemistry A*, *114*(31), 8106–8113. https://doi.org/10.1021/jp103907c

Ehn, M., Thornton, J. A., Kleist, E., Sipilä, M., Junninen, H., Pullinen, I., et al. (2014). A large source of low-volatility secondary organic aerosol. *Nature*, *506*(7489), 476–479. https://doi.org/10.1038/nature13032

Enami, S., Hoffmann, M. R., & Colussi, A. J. (2017). Criegee intermediates react with levoglucosan on water. *The Journal of Physical Chemistry Letters*, *8*(16), 3888–3894. https://doi.org/10.1021/acs.jpclett.7b01665

Ervens, B., Turpin, B. J., & Weber, R. J. (2011). Secondary organic aerosol formation in cloud droplets and aqueous particles (aqSOA): A review of laboratory, field and model studies. *Atmospheric Chemistry and Physics*, *11*(21), 11069–11102. https://doi.org/10.5194/acp-11-11069-2011

Eugene, A. J., Pillar, E. A., Colussi, A. J., & Guzman, M. I. (2018). Enhanced acidity of acetic and pyruvic acids on the surface of water. *Langmuir*, *34*(31), 9307–9313. https://doi.org/10.1021/acs.langmuir.8b01606

Evans, M. G., & Polanyi, M. (1936). Further considerations on the thermodynamics of chemical equilibria and reaction rates. *Transactions of the Faraday Society*, *32*(0), 1333–1360. https://doi.org/10.1039/TF9363201333

Facchini, M. C., Mircea, M., Fuzzi, S., & Charlson, R. J. (1999). Cloud albedo enhancement by surface-active organic solutes in growing droplets. *Nature*, *401*(6750), 257–259. https://doi.org/10.1038/45758

Fang, X., Hu, M., Shang, D., Tang, R., Shi, L., Olenius, T., et al. (2020). Observational evidence for the involvement of dicarboxylic acids in particle nucleation. *Environmental Science and Technology Letters*, *7*(6), 388–394. https://doi.org/10.1021/acs.estlett.0c00270

Forestieri, S. D., Staudt, S. M., Kuborn, T. M., Faber, K., Ruehl, C. R., Bertram, T. H., & Cappa, C. D. (2018). Establishing the impact of model surfactants on cloud condensation nuclei activity of sea spray aerosol mimics. *Atmospheric Chemistry and Physics*, *18*(15), 10985–11005. https://doi.org/10.5194/acp-18-10985-2018

Forster, P., Storelvmo, T., Armour, K., Collins, W., Dufresne, J.-L., Frame, D., et al. (2021). The Earth's energy budget, climate feedbacks, and climate sensitivity. In V. Masson-Delmotte, P. Zhai, A. Pirani, S. L. Connors, C. Péan, S. Berger, et al. (Eds.), *Climate change 2021: The physical science basis. Contribution of working group I to the sixth assessment report of the Intergovernmental panel on climate change*. Cambridge University Press. Retrieved from https://www.ipcc.ch/report/ar6/wg1/downloads/report/IPCC_AR6_WGI_Chapter_07.pdf

Froyd, K. D., Murphy, S. M., Murphy, D. M., De Gouw, J. A., Eddingsaas, N. C., & Wennberg, P. O. (2010). Contribution of isoprene-derived organosulfates to free tropospheric aerosol mass. *Proceedings of the National Academy of Sciences U.S.A.*, *107*(50), 21360–21365. https://doi.org/10.1073/pnas.1012561107

Fulcher, G. S. (1925). Analysis of recent measurements of the viscosity of glasses. *Journal of the American Ceramic Society*, *8*(6), 339–355. https://doi.org/10.1111/j.1151-2916.1925.tb16731.x

Glasius, M., & Goldstein, A. H. (2016). Recent discoveries and future challenges in atmospheric organic chemistry. *Environmental Science & Technology*, *50*(6), 2754–2764. https://doi.org/10.1021/acs.est.5b05105

Gordon, B. P., Moore, F. G., Scatena, L., & Richmond, G. L. (2019). On the rise: Experimental and computational VSFS studies of pyruvic acid and its surface active oligomer species at the air-water interface. *The Journal of Physical Chemistry A*, *123*, 10609–10619. https://doi.org/10.1021/acs.jpca.9b08854

Gordon, H., Kirkby, J., Baltensperger, U., Bianchi, F., Breitenlechner, M., Curtius, J., et al. (2017). Causes and importance of new particle formation in the present-day and preindustrial atmospheres. *Journal of Geophysical Research: Atmospheres*, *122*(16), 8739–8760. https://doi.org/10.1002/2017JD026844

Grove, S. F., Lee, A., Lewis, T., Stewart, C. M., Chen, H., & Hoover, D. G. (2006). Inactivation of foodborne viruses of significance by high pressure and other processes. *Journal of Food Protection*, *69*(4), 957–968. https://doi.org/10.4315/0362-028X-69.4.957

Hartikainen, A., Yli-Pirilä, P., Tiitta, P., Leskinen, A., Kortelainen, M., Orasche, J., et al. (2018). Volatile organic compounds from logwood combustion: Emissions and transformation under dark and photochemical aging conditions in a smog chamber. *Environmental Science & Technology*, *52*(8), 4979–4988. https://doi.org/10.1021/acs.est.7b06269

Hazen, R. M., Boctor, N., Brandes, J. A., Cody, G. D., Hemley, R. J., Sharma, A., & Yoder, H. S. (2002). High pressure and the origin of life. *Journal of Physics: Condensed Matter*, *14*(44), 11489–11494. https://doi.org/10.1088/0953-8984/14/44/504

Hede, T., Li, X., Leck, C., Tu, Y., & Ågren, H. (2011). Model HULIS compounds in nanoaerosol clusters – Investigations of surface tension and aggregate formation using molecular dynamics simulations. *Atmospheric Chemistry and Physics*, *11*(13), 6549–6557. https://doi.org/10.5194/acp-11-6549-2011

Hennigan, C. J., Westervelt, D. M., Riipinen, I., Engelhart, G. J., Lee, T., Collett, J. L., Jr., et al. (2012). New particle formation and growth in biomass burning plumes: An important source of cloud condensation nuclei. Geophysical Research Letters, *39*(9). https://doi.org/10.1029/2012GL050930

Herbst, C. A., Cook, R. L., & King, H. E., Jr. (1993). High-pressure viscosity of glycerol measured by centrifugal-force viscometry. *Nature*, *361*(6412), 518–520. https://doi.org/10.1038/361518a0

Herrmann, H., Schaefer, T., Tilgner, A., Styler, S. A., Weller, C., Teich, M., & Otto, T. (2015). Tropospheric aqueous-phase chemistry: Kinetics, mechanisms, and its coupling to a changing gas phase. *Chemical Reviews*, *115*(10), 4259–4334. https://doi.org/10.1021/cr500447k

Hodzic, A., Jimenez, J. L., Madronich, S., Canagaratna, M. R., DeCarlo, P. F., Kleinman, L., & Fast, J. (2010). Modeling organic aerosols in a megacity: Potential contribution of semi-volatile and intermediate volatility primary organic compounds to secondary organic aerosol formation. *Atmospheric Chemistry and Physics*, *10*(12), 5491–5514. https://doi.org/10.5194/acp-10-5491-2010

Houk, K. N., Jabbari, A., Hall, H. K., & Alemán, C. (2008). Why δ-valerolactone polymerizes and γ-butyrolactone does not. *Journal of Organic Chemistry*, *73*(7), 2674–2678. https://doi.org/10.1021/jo702567v

Hritz, A. D., Raymond, T. M., & Dutcher, D. D. (2016). A method for the direct measurement of surface tension of collected atmospherically relevant aerosol particles using atomic force microscopy. *Atmospheric Chemistry and Physics*, *16*(15), 9761–9769. https://doi.org/10.5194/acp-16-9761-2016

Hu, D., Liu, D., Kong, S., Zhao, D., Wu, Y., Li, S., et al. (2021). Direct quantification of droplet activation of ambient black carbon under water supersaturation. *Journal of Geophysical Research: Atmospheres*, *126*, e2021JD034649. https://doi.org/10.1029/2021JD034649

Hu, W. W., Campuzano-Jost, P., Palm, B. B., Day, D. A., Ortega, A. M., Hayes, P. L., et al. (2015). Characterization of a real-time tracer for isoprene epoxydiols-derived secondary organic aerosol (IEPOX-SOA) from aerosol mass spectrometer measurements. *Atmospheric Chemistry and Physics*, *15*(20), 11807–11833. https://doi.org/10.5194/acp-15-11807-2015

Ingold, K. U. (1961). Inhibition of the autoxidation of organic substances in the liquid phase. *Chemical Reviews*, *61*(6), 563–589. https://doi.org/10.1021/cr60214a002

Isaacs, N. S. (1997). Chemical transformations. In W. B. Holzapfel, & N. S. Isaacs (Eds.), *High pressure techniques in chemistry and physics: A practical approach*. Oxford University. Retrieved from https://catalog.lib.ncsu.edu/catalog/NCSU962634

Jang, M., Czoschke, N., Lee, S., & Kamens, R. (2002). Heterogeneous atmospheric aerosol production by acid-catalyzed particle-phase reactions. *Science*, *298*(5594), 814–817. https://doi.org/10.1126/science.1075798

Jenner, G. (1999). Effect of high pressure on Michael and Henry reactions between ketones and nitroalkanes. *New Journal of Chemistry*, *23*(5), 525–529. https://doi.org/10.1039/A900899C

Jenner, G. (2001). High pressure mechanistic diagnosis in Baeyer–Villiger oxidation of aliphatic ketones. *Tetrahedron Letters*, *42*(51), 8969–8971. https://doi.org/10.1016/S0040-4039(01)01955-4

Johansson, K. O., Head-Gordon, M. P., Schrader, P. E., Wilson, K. R., & Michelsen, H. A. (2018). Resonance-stabilized hydrocarbon-radical chain reactions may explain soot inception and growth. *Science*, *361*(6406), 997–1000. https://doi.org/10.1126/science.aat3417

Kaptay, G. (2012). The Gibbs equation versus the Kelvin and the Gibbs-Thomson equations to describe nucleation and equilibrium of nano-materials. *Journal of Nanoscience and Nanotechnology*, *12*(3), 2625–2633. https://doi.org/10.1166/jnn.2012.5774

Kasparoglu, S., Li, Y., Shiraiwa, M., & Petters, M. D. (2021). Toward closure between predicted and observed particle viscosity over a wide range of temperatures and relative humidity. *Atmospheric Chemistry and Physics*, *21*(2), 1127–1141. https://doi.org/10.5194/acp-21-1127-2021

Kerminen, V.-M., Chen, X., Vakkari, V., Petäjä, T., Kulmala, M., & Bianchi, F. (2018). Atmospheric new particle formation and growth: Review of field observations. *Environmental Research Letters*, *13*(10), 103003. https://doi.org/10.1088/1748-9326/aadf3c

Kirkby, J., Duplissy, J., Sengupta, K., Frege, C., Gordon, H., Williamson, C., et al. (2016). Ion-induced nucleation of pure biogenic particles. *Nature*, *533*(7604), 521–526. https://doi.org/10.1038/nature17953

Klärner, F.-G., & Wurche, F. (2000). The effect of pressure on organic reactions. *Journal für Praktische Chemie*, *342*(7), 609–636. https://doi.org/10.1002/1521-3897(200009)342:7<609::AID-PRAC609>3.0.CO;2-Z

Korosi, G., & Kovats, E. S. (1981). Density and surface tension of 83 organic liquids. *Journal of Chemical & Engineering Data*, *26*(3), 323–332. https://doi.org/10.1021/je00025a032

Koskikallio, J., & Whalley, E. (1959). Pressure effect and mechanism in acid catalysis. Part 3.—Hydrolysis of epoxides. *Transactions of the Faraday Society*, *55*(0), 815–823. https://doi.org/10.1039/TF9595500815

Kovač, K., Diez-Valcarce, M., Hernandez, M., Raspor, P., & Rodríguez-Lázaro, D. (2010). High hydrostatic pressure as emergent technology for the elimination of foodborne viruses. *Trends in Food Science & Technology*, *21*(11), 558–568. https://doi.org/10.1016/j.tifs.2010.08.002

Kreidenweis, S. M., Koehler, K., DeMott, P. J., Prenni, A. J., Carrico, C., & Ervens, B. (2005). Water activity and activation diameters from hygroscopicity data – Part I: Theory and application to inorganic salts. *Atmospheric Chemistry and Physics*, *5*(5), 1357–1370. https://doi.org/10.5194/acp-5-1357-2005

Kristensen, T. B., Falk, J., Lindgren, R., Andersen, C., Malmborg, V. B., Eriksson, A. C., et al. (2021). Properties and emission factors of cloud condensation nuclei from biomass cookstoves – Observations of a strong dependency on potassium content in the fuel. *Atmospheric Chemistry and Physics*, *21*(10), 8023–8044. https://doi.org/10.5194/acp-21-8023-2021

Kulmala, M., Vehkamäki, H., Petäjä, T., Dal Maso, M., Lauri, A., Kerminen, V.-M., et al. (2004). Formation and growth rates of ultrafine atmospheric particles: A review of observations. *Journal of Aerosol Science*, *35*(2), 143–176. https://doi.org/10.1016/j.jaerosci.2003.10.003

Kürten, A., Bergen, A., Heinritzi, M., Leiminger, M., Lorenz, V., Piel, F., et al. (2016). Observation of new particle formation and measurement of sulfuric acid, ammonia, amines and highly oxidized organic molecules at a rural site in central Germany. *Atmospheric Chemistry and Physics*, *16*(19), 12793–12813. https://doi.org/10.5194/acp-16-12793-2016

Kürten, A., Bianchi, F., Almeida, J., Kupiainen-Määttä, O., Dunne, E. M., Duplissy, J., et al. (2016). Experimental particle formation rates spanning tropospheric sulfuric acid and ammonia abundances, ion production rates, and temperatures. *Journal of Geophysical Research: Atmospheres*, *121*(20), 12377–12400. https://doi.org/10.1002/2015JD023908

Kurtén, T., Loukonen, V., Vehkamäki, H., & Kulmala, M. (2008). Amines are likely to enhance neutral and ion-induced sulfuric acid-water nucleation in the atmosphere more effectively than ammonia. *Atmospheric Chemistry and Physics*, *8*(14), 4095–4103. https://doi.org/10.5194/acp-8-4095-2008

Laaksonen, A., McGraw, R., & Vehkamäki, H. (1999). Liquid-drop formalism and free-energy surfaces in binary homogeneous nucleation theory. *The Journal of Chemical Physics*, *111*(5), 2019–2027. https://doi.org/10.1063/1.479470

Leung, K. K., Schnitzler, E. G., Dastanpour, R., Rogak, S. N., Jäger, W., & Olfert, J. S. (2017). Relationship between coating-induced soot aggregate restructuring and primary particle number. *Environmental Science & Technology*, *51*(15), 8376–8383. https://doi.org/10.1021/acs.est.7b01140

Liang, X., Haynes, B. S., & Montoya, A. (2018). Acid-catalyzed ring opening of furan in aqueous solution. *Energy & Fuels*, *32*(4), 4139–4148. https://doi.org/10.1021/acs.energyfuels.7b03239

Lim, Y. B., Tan, Y., Perri, M. J., Seitzinger, S. P., & Turpin, B. J. (2010). Aqueous chemistry and its role in secondary organic aerosol (SOA) formation. *Atmospheric Chemistry and Physics*, *10*(21), 10521–10539. https://doi.org/10.5194/acp-10-10521-2010

Lin, Y.-H., Zhang, H., Pye, H. O. T., Zhang, Z., Marth, W. J., Park, S., et al. (2013). Epoxide as a precursor to secondary organic aerosol formation from isoprene photooxidation in the presence of nitrogen oxides. *Proceedings of the National Academy of Sciences U.S.A.*, *110*(17), 6718–6723. https://doi.org/10.1073/pnas.1221150110

Liu, H., & Cao, G. (2016). Effectiveness of the Young-Laplace equation at nanoscale. *Scientific Reports*, *6*(1), 23936. https://doi.org/10.1038/srep23936

Loeffler, K. W., Koehler, C. A., Paul, N. M., & De Haan, D. O. (2006). Oligomer formation in evaporating aqueous glyoxal and methyl glyoxal solutions. *Environmental Science & Technology*, *40*(20), 6318–6323. https://doi.org/10.1021/es060810w

Ma, X., Zangmeister, C. D., Gigault, J., Mulholland, G. W., & Zachariah, M. R. (2013). Soot aggregate restructuring during water processing. *Journal of Aerosol Science*, *66*, 209–219. https://doi.org/10.1016/j.jaerosci.2013.08.001

Malila, J., & Prisle, N. L. (2018). A monolayer partitioning scheme for droplets of surfactant solutions. *Journal of Advances in Modeling Earth Systems*, *10*(12), 3233–3251. https://doi.org/10.1029/2018MS001456

Marcus, Y. (1998). *The properties of solvents*. Wiley. Retrieved from https://catalog.lib.ncsu.edu/catalog/NCSU1038777

Marsh, A., Petters, S. S., Rothfuss, N. E., Rovelli, G., Song, Y. C., Reid, J. P., & Petters, M. D. (2018). Amorphous phase state diagrams and viscosity of ternary aqueous organic/organic and inorganic/organic mixtures. *Physical Chemistry Chemical Physics*, *20*(22), 15086–15097. https://doi.org/10.1039/C8CP00760H

Matsunaga, A., & Ziemann, P. J. (2010). Yields of β-hydroxynitrates, dihydroxynitrates, and trihydroxynitrates formed from OH radical-initiated reactions of 2-methyl-1-alkenes. *Proceedings of the National Academy of Sciences U.S.A.*, *107*(15), 6664–6669. https://doi.org/10.1073/pnas.0910585107

Maxut, A., Nozière, B., Fenet, B., & Mechakra, H. (2015). Formation mechanisms and yields of small imidazoles from reactions of glyoxal with NH_4^+ in water at neutral pH. *Physical Chemistry Chemical Physics*, *17*(31), 20416–20424. https://doi.org/10.1039/C5CP03113C

McGraw, R., & Wang, J. (2021). Surfactants and cloud droplet activation: A systematic extension of Köhler theory based on analysis of droplet stability. *The Journal of Chemical Physics*, *154*(2), 024707. https://doi.org/10.1063/5.0031436

McRae, O., Mead, K. R., & Bird, J. C. (2021). Aerosol agitation: Quantifying the hydrodynamic stressors on particulates encapsulated in small droplets. *Physical Review Fluids*, *6*(3), L031601. https://doi.org/10.1103/PhysRevFluids.6.L031601

Minerath, E. C., & Elrod, M. J. (2009). Assessing the potential for diol and hydroxy sulfate ester formation from the reaction of epoxides in tropospheric aerosols. *Environmental Science & Technology*, *43*(5), 1386–1392. https://doi.org/10.1021/es8029076

Mohr, C., Thornton, J. A., Heitto, A., Lopez-Hilfiker, F. D., Lutz, A., Riipinen, I., et al. (2019). Molecular identification of organic vapors driving atmospheric nanoparticle growth. *Nature Communications*, *10*(1), 4442. https://doi.org/10.1038/s41467-019-12473-2

Nakao, S., Tang, P., Tang, X., Clark, C. H., Qi, L., Seo, E., et al. (2013). Density and elemental ratios of secondary organic aerosol: Application of a density prediction method. *Atmospheric Environment*, *68*, 273–277. https://doi.org/10.1016/j.atmosenv.2012.11.006

Nguyen, T. B., Bates, K. H., Crounse, J. D., Schwantes, R. H., Zhang, X., Kjaergaard, H. G., et al. (2015). Mechanism of the hydroxyl radical oxidation of methacryloyl peroxynitrate (MPAN) and its pathway toward secondary organic aerosol formation in the atmosphere. *Physical Chemistry Chemical Physics*, *17*(27), 17914–17926. https://doi.org/10.1039/C5CP02001H

Nguyen, T. B., Coggon, M. M., Bates, K. H., Zhang, X., Schwantes, R. H., Schilling, K. A., et al. (2014). Organic aerosol formation from the reactive uptake of isoprene epoxydiols (IEPOX) onto non-acidified inorganic seeds. *Atmospheric Chemistry and Physics*, *14*(7), 3497–3510. https://doi.org/10.5194/acp-14-3497-2014

Nguyen, T. K. V., Petters, M. D., Suda, S. R., Guo, H., Weber, R. J., & Carlton, A. G. (2014). Trends in particle-phase liquid water during the Southern oxidant and aerosol study. *Atmospheric Chemistry and Physics*, *14*(20), 10911–10930. https://doi.org/10.5194/acp-14-10911-2014

Nozière, B., Baduel, C., & Jaffrezo, J.-L. (2014). The dynamic surface tension of atmospheric aerosol surfactants reveals new aspects of cloud activation. *Nature Communications*, *5*, 3333. https://doi.org/10.1038/ncomms4335

Nozière, B., Dziedzic, P., & Córdova, A. (2010). Inorganic ammonium salts and carbonate salts are efficient catalysts for aldol condensation in atmospheric aerosols. *Physical Chemistry Chemical Physics*, *12*(15), 3864–3872. https://doi.org/10.1039/B924443C

Nozière, B., Fache, F., Maxut, A., Fenet, B., Baudouin, A., Fine, L., & Ferronato, C. (2018). The hydrolysis of epoxides catalyzed by inorganic ammonium salts in water: Kinetic evidence for hydrogen bond catalysis. *Physical Chemistry Chemical Physics*, *20*(3), 1583–1590. https://doi.org/10.1039/C7CP06790A

O'Dowd, C. D., Jimenez, J. L., Bahreini, R., Flagan, R. C., Seinfeld, J. H., Hämeri, K., et al. (2002). Marine aerosol formation from biogenic iodine emissions. *Nature*, *417*(6889), 632–636. https://doi.org/10.1038/nature00775

Oppolzer, W. (1991). Combining C–C pi-Bonds. In B. M. Trost, I. Fleming, & L. A. Paquette (Eds.), *Comprehensive organic synthesis : Selectivity, strategy, & efficiency in modern organic chemistry* (Vol. 5). Pergamon. Retrieved from https://catalog.lib.ncsu.edu/catalog/NCSU773032

Ovadnevaite, J., Zuend, A., Laaksonen, A., Sanchez, K. J., Roberts, G., Ceburnis, D., et al. (2017). Surface tension prevails over solute effect in organic-influenced cloud droplet activation. *Nature*, *546*(7660), 637–641. https://doi.org/10.1038/nature22806

Paulot, F., Crounse, J. D., Kjaergaard, H. G., Kürten, A., St Clair, J. M., Seinfeld, J. H., & Wennberg, P. O. (2009). Unexpected epoxide formation in the gas-phase photooxidation of isoprene. *Science*, *325*(5941), 730–733. https://doi.org/10.1126/science.1172910

Perkins, R. J., Shoemaker, R. K., Carpenter, B. K., & Vaida, V. (2016). Chemical equilibria and kinetics in aqueous solutions of zymonic acid. *The Journal of Physical Chemistry A*, *120*(51), 10096–10107. https://doi.org/10.1021/acs.jpca.6b10526

Petters, M. D., & Kasparoglu, S. (2020). Predicting the influence of particle size on the glass transition temperature and viscosity of secondary organic material. *Scientific Reports*, *10*(1), 15170. https://doi.org/10.1038/s41598-020-71490-0

Petters, M. D., & Kreidenweis, S. M. (2013). A single parameter representation of hygroscopic growth and cloud condensation nucleus activity – Part 3: Including surfactant partitioning. *Atmospheric Chemistry and Physics*, *13*(2), 1081–1091. https://doi.org/10.5194/acp-13-1081-2013

Petters, S. S., Cui, T., Zhang, Z., Gold, A., McNeill, V. F., Surratt, J. D., & Turpin, B. J. (2021). Organosulfates from dark aqueous reactions of isoprene-derived epoxydiols under cloud and fog conditions: Kinetics, mechanism, and effect of reaction environment on regioselectivity of sulfate addition. *ACS Earth and Space Chemistry*, *5*, 474–486. https://doi.org/10.1021/acsearthspacechem.0c00293

Petters, S. S., Hilditch, T. G., Tomaz, S., Miles, R. E. H., Reid, J. P., & Turpin, B. J. (2020). Volatility change during droplet evaporation of pyruvic acid. *ACS Earth and Space Chemistry*, *4*, 741–749. https://doi.org/10.1021/acsearthspacechem.0c00044

Petters, S. S., Kreidenweis, S. M., Grieshop, A. P., Ziemann, P. J., & Petters, M. D. (2019). Temperature- and humidity-dependent phase states of secondary organic aerosols. *Geophysical Research Letters*, *46*(2), 1005–1013. https://doi.org/10.1029/2018GL080563

Petters, S. S., & Petters, M. D. (2016). Surfactant effect on cloud condensation nuclei for two-component internally mixed aerosols. *Journal of Geophysical Research: Atmospheres*, *121*(4), 1878–1895. https://doi.org/10.1002/2015JD024090

Pierce, J. R., Riipinen, I., Kulmala, M., Ehn, M., Petäjä, T., Junninen, H., et al. (2011). Quantification of the volatility of secondary organic compounds in ultrafine particles during nucleation events. *Atmospheric Chemistry and Physics*, *11*(17), 9019–9036. https://doi.org/10.5194/acp-11-9019-2011

Pospisilova, V., Lopez-Hilfiker, F. D., Bell, D. M., Elhaddad, I., Mohr, C., Huang, W., et al. (2020). On the fate of oxygenated organic molecules in atmospheric aerosol particles. *Science Advances*, *6*(11), eaax8922. https://doi.org/10.1126/sciadv.aax8922

Prisle, N. L., Raatikainen, T., Sorjamaa, R., Svenningsson, B., Laaksonen, A., & Bilde, M. (2008). Surfactant partitioning in cloud droplet activation: A study of C8, C10, C12 and C14 normal fatty acid sodium salts. *Tellus: Series B*, *60*(3), 416–431. https://doi.org/10.1111/j.1600-0889.2008.00352.x

Pruppacher, H. R., & Klett, J. D. (2010). *Microphysics of clouds and precipitation*. Springer. https://doi.org/10.1007/978-0-306-48100-0

Pye, H. O. T., Nenes, A., Alexander, B., Ault, A. P., Barth, M. C., Clegg, S. L., et al. (2020). The acidity of atmospheric particles and clouds. *Atmospheric Chemistry and Physics*, *20*(8), 4809–4888. https://doi.org/10.5194/acp-20-4809-2020

Rastak, N., Pajunoja, A., Acosta Navarro, J. C., Ma, J., Song, M., Partridge, D. G., et al. (2017). Microphysical explanation of the RH-dependent water affinity of biogenic organic aerosol and its importance for climate. *Geophysical Research Letters*, *44*(10), 5167–5177. https://doi.org/10.1002/2017GL073056

Reid, J. P., Bertram, A. K., Topping, D. O., Laskin, A., Martin, S. T., Petters, M. D., et al. (2018). The viscosity of atmospherically relevant organic particles. *Nature Communications*, *9*(1), 956. https://doi.org/10.1038/s41467-018-03027-z

Renbaum-Wolff, L., Grayson, J. W., Bateman, A. P., Kuwata, M., Sellier, M., Murray, B. J., et al. (2013). Viscosity of α-pinene secondary organic material and implications for particle growth and reactivity. *Proceedings of the National Academy of Sciences U.S.A.*, *110*(20), 8014–8019. https://doi.org/10.1073/pnas.1219548110

Renbaum-Wolff, L., Song, M., Marcolli, C., Zhang, Y., Liu, P. F., Grayson, J. W., et al. (2016). Observations and implications of liquid–liquid phase separation at high relative humidities in secondary organic material produced by α-pinene ozonolysis without inorganic salts. *Atmospheric Chemistry and Physics*, *16*(12), 7969–7979. https://doi.org/10.5194/acp-16-7969-2016

Richard, A. J., & Rogers, K. S. (1971). The isothermal compressibility of organic liquids by ultracentrifugation. correlation with surface tension. *Canadian Journal of Chemistry*, *49*(24), 3956–3959. https://doi.org/10.1139/v71-662

Riva, M., Sun, J., McNeill, V. F., Ragon, C., Perrier, S., Rudich, Y., et al. (2021). High pressure inside nanometer-sized particles influences the rate and products of chemical reactions. *Environmental Science & Technology*, *55*, 7786–7793. https://doi.org/10.1021/acs.est.0c07386

Rothfuss, N. E., & Petters, M. D. (2017). Characterization of the temperature and humidity-dependent phase diagram of amorphous nanoscale organic aerosols. *Physical Chemistry Chemical Physics*, *19*(9), 6532–6545. https://doi.org/10.1039/C6CP08593H

Rowlinson, J. S., & Widom, B. (1982). *Molecular theory of Capillarity*. Dover. Retrieved from https://catalog.lib.ncsu.edu/catalog/NCSU570611

Ruehl, C. R., Davies, J. F., & Wilson, K. R. (2016). An interfacial mechanism for cloud droplet formation on organic aerosols. *Science*, *351*(6280), 1447–1450. https://doi.org/10.1126/science.aad4889

Schmelzer, J. W. P., Gutzow, I., & Mazurin, O. V. (2011). *Glasses and the glass transition*. Wiley-VCH Verlag. Retrieved from https://catalog.lib.ncsu.edu/catalog/NCSU4252002

Schmelzer, J. W. P., Zanotto, E. D., & Fokin, V. M. (2005). Pressure dependence of viscosity. *The Journal of Chemical Physics*, *122*(7), 074511. https://doi.org/10.1063/1.1851510

Schulz, C., Schneider, J., Holanda, B. A., Appel, O., Costa, A., De Sá, S. S., et al. (2018). Aircraft-based observations of isoprene-epoxydiol-derived secondary organic aerosol (IEPOX-SOA) in the tropical upper troposphere over the Amazon region. *Atmospheric Chemistry and Physics*, *18*(20), 14979–15001. https://doi.org/10.5194/acp-18-14979-2018

Singh, L. P., Issenmann, B., & Caupin, F. (2017). Pressure dependence of viscosity in supercooled water and a unified approach for thermodynamic and dynamic anomalies of water. *Proceedings of the National Academy of Sciences U.S.A.*, *114*(17), 4312–4317. https://doi.org/10.1073/pnas.1619501114

Sipilä, M., Berndt, T., Petäjä, T., Brus, D., Vanhanen, J., Stratmann, F., et al. (2010). The role of sulfuric acid in atmospheric nucleation. *Science*, *327*(5970), 1243–1246. https://doi.org/10.1126/science.1180315

Sipilä, M., Sarnela, N., Jokinen, T., Henschel, H., Junninen, H., Kontkanen, J., et al. (2016). Molecular-scale evidence of aerosol particle formation via sequential addition of HIO_3. *Nature*, *537*(7621), 532–534. https://doi.org/10.1038/nature19314

Su, H., Cheng, Y., & Pöschl, U. (2020). New multiphase chemical processes influencing atmospheric aerosols, air quality, and climate in the Anthropocene. *Accounts of Chemical Research*, *53*(10), 2034–2043. https://doi.org/10.1021/acs.accounts.0c00246

Sumi, H. (1991). Theory on reaction rates in nonthermalized steady states during conformational fluctuations in viscous solvents. *The Journal of Physical Chemistry*, *95*(8), 3334–3350. https://doi.org/10.1021/j100161a068

Surratt, J. D., Chan, A. W. H., Eddingsaas, N. C., Chan, M., Loza, C. L., Kwan, A. J., et al. (2010). Reactive intermediates revealed in secondary organic aerosol formation from isoprene. *Proceedings of the National Academy of Sciences U.S.A.*, *107*(15), 6640–6645. https://doi.org/10.1073/pnas.0911114107

Tiab, D., & Donaldson, E. C. (2016). Introduction to petroleum geology. In D. Tiab, & E. C. Donaldson (Eds.), *Petrophysics* (4th ed., pp. 23–66). Gulf Professional Publishing. https://doi.org/10.1016/B978-0-12-803188-9.00002-4

Tomaz, S., Cui, T., Chen, Y., Sexton, K. G., Roberts, J. M., Warneke, C., et al. (2018). Photochemical cloud processing of primary wildfire emissions as a potential source of secondary organic aerosol. *Environmental Science & Technology*, *52*(19), 11027–11037. https://doi.org/10.1021/acs.est.8b03293

Tröstl, J., Chuang, W. K., Gordon, H., Heinritzi, M., Yan, C., Molteni, U., et al. (2016). The role of low-volatility organic compounds in initial particle growth in the atmosphere. *Nature*, *533*(7604), 527–531. https://doi.org/10.1038/nature18271

Van Eldik, R., & Hubbard, C. D. (1997). *Chemistry under extreme and non-classical conditions*. Wiley. Retrieved from https://catalog.lib.ncsu.edu/catalog/NCSU962452

Van Eldik, R., & Kelm, H. (1980). Interpretation of the volume of activation of inorganic reactions in solution. *Review of Physical Chemistry of Japan*, *50*, 185–206.

Virtanen, A., Joutsensaari, J., Koop, T., Kannosto, J., Yli-Pirilä, P., Leskinen, J., et al. (2010). An amorphous solid state of biogenic secondary organic aerosol particles. *Nature*, *467*(7317), 824–827. https://doi.org/10.1038/nature09455

Wang, M., Kong, W., Marten, R., He, X.-C., Chen, D., Pfeifer, J., et al. (2020). Rapid growth of new atmospheric particles by nitric acid and ammonia condensation. *Nature*, *581*(7807), 184–189. https://doi.org/10.1038/s41586-020-2270-4

Wei, H., Vejerano, E. P., Leng, W., Huang, Q., Willner, M. R., Marr, L. C., & Vikesland, P. J. (2018). Aerosol microdroplets exhibit a stable pH gradient. *Proceedings of the National Academy of Sciences U.S.A.*, *115*(28), 7272–7277. https://doi.org/10.1073/pnas.1720488115

Wex, H., Stratmann, F., Hennig, T., Hartmann, S., Niedermeier, D., Nilsson, E., et al. (2008). Connecting hygroscopic growth at high humidities to cloud activation for different particle types. *Environmental Research Letters*, *3*(3), 035004. https://doi.org/10.1088/1748-9326/3/3/035004

Wex, H., Stratmann, F., Topping, D., & McFiggans, G. (2008). The Kelvin versus the Raoult term in the Köhler equation. *Journal of the Atmospheric Sciences*, *65*(12), 4004–4016. https://doi.org/10.1175/2008JAS2720.1

Whalley, E. (1959). Pressure effect and mechanism in acid catalysis. Part 1. *Transactions of the Faraday Society*, *55*(0), 798–808. https://doi.org/10.1039/TF9595500798

Xu, L., Guo, H., Boyd, C. M., Klein, M., Bougiatioti, A., Cerully, K. M., et al. (2015). Effects of anthropogenic emissions on aerosol formation from isoprene and monoterpenes in the southeastern United States. *Proceedings of the National Academy of Sciences U.S.A.*, *112*(1), 37–42. https://doi.org/10.1073/pnas.1417609112

Yamashita, K., Yamamoto, K., & Kadokawa, J. (2014). Acid-catalyzed ring-opening polymerization of γ-butyrolactone under high-pressure conditions. *Chemistry Letters*, *43*(2), 213–215. https://doi.org/10.1246/cl.130952

Yao, L., Garmash, O., Bianchi, F., Zheng, J., Yan, C., Kontkanen, J., et al. (2018). Atmospheric new particle formation from sulfuric acid and amines in a Chinese megacity. *Science*, *361*(6399), 278–281. https://doi.org/10.1126/science.aao4839

Yaws, C. L. (2003). *Yaws' handbook of thermodynamic and physical properties of chemical compounds*. Knovel. Retrieved from https://catalog.lib.ncsu.edu/catalog/NCSU5251508.,

Zhao, J., Smith, J. N., Eisele, F. L., Chen, M., Kuang, C., & McMurry, P. H. (2011). Observation of neutral sulfuric acid-amine containing clusters in laboratory and ambient measurements. *Atmospheric Chemistry and Physics*, *11*(21), 10823–10836. https://doi.org/10.5194/acp-11-10823-2011

Ziemann, P. J., & Atkinson, R. (2012). Kinetics, products, and mechanisms of secondary organic aerosol formation. *Chemical Society Reviews*, *41*(19), 6582–6605. https://doi.org/10.1039/C2CS35122F